# Passive mode-locking of p-doped quantum dot semiconductor lasers

**D Auth[1], V V Korenev[2], A V Savelyev[2], M V Maximov[2], A E Zhukov[3], and S Breuer[1]**

[1] Institute of Applied Physics, Technische Universität Darmstadt, Schlossgartenstraße 7, 64289 Darmstadt, Germany
[2] Alferov University RAS, ul. Khlopina 8/3, 194021 St. Petersburg, Russia
[3] National Research University Higher School of Economics, Soyuza Pechatnikov 16, 190008 St. Petersburg, Russia

E-mail: `stefan.breuer@physik.tu-darmstadt.de`

**Abstract.** Quantum dot based monolithic edge-emitting semiconductor lasers at 1.25 $\mu$m are ideal sources for the generation of broad optical frequency combs for optical communication applications. In this work, InAs/InGaAs quantum dot lasers with different total laser length to absorber length ratio and with different p-doping concentrations in the GaAs barrier sections are investigated experimentally in dependence on the gain injection current and absorber reverse bias voltage. A smaller mode-locking area is found for the p-doped device in dependence on the laser biasing conditions. For the undoped active region 1.3 ps short pulse widths at a pulse repetition rate of 20 GHz with a pulse-to-pulse timing jitter of 111 fs are reported for an absorber section length of 12% to the total cavity length. For an undoped and p-doped device short pulse emission between 2.5 ps and 5.5 ps is attained and a shorter absorber section length of 8% or 5%.

## 1. Introduction

Passively mode-locked semiconductor quantum dot lasers generating picosecond short optical pulses at high pulse repetition rates spectrally centered at 1.25 $\mu$m are ideal sources for telecommunication applications [1, 2, 3] or master oscillator power amplifier set-ups [4] for two-photon excitation fluorescence microscopy due to the high penetration depth of this wavelength into organic tissues [5]. Mode-locked semiconductor quantum dot lasers offer compact size and low energy consumption [1, 2, 3, 6, 7]. Optical pulse generation in quantum dot lasers benefits from broad gain spectra, due to the inhomogeneous broadening of the dots [8, 9, 10], ultra-fast carrier dynamics [11], modal gain saturating abruptly with carrier density [12, 13] and easily saturable absorbers [14]. For quantum dot lasers, pulse widths below 1 ps [15, 16, 17] and low pulse-to-pulse timing jitter have been reported for devices with different geometries, including multi-section and tapered structures [18, 19, 20, 21, 22]. For quantum dot lasers directly grown on silicon, longer absorber section lengths yield shorter pulses [23]. Modifying the p-doping in the active region of quantum dot lasers resulted in a higher modal gain at a fixed current density in mode-locked quantum dot on silicon lasers [24] and in broad area quantum dot lasers [24, 25].

In this work, the impact of total laser length to absorber length ratio and p-doping level onto the pulsed emission of 2 mm long two-section passively mode-locked InAs/InGaAs quantum dot

Content from this work may be used under the terms of the Creative Commons Attribution 3.0 licence. Any further distribution of this work must maintain attribution to the author(s) and the title of the work, journal citation and DOI.
Published under licence by IOP Publishing Ltd

lasers is studied experimentally. Shortest pulse widths and optimum pulse train stability are quantified in dependence on the gain injection current and absorber reverse bias voltage.

## 2. Quantum dot laser devices and experiment

The investigated two-section quantum dot laser devices consist of 10 layers of InAs/InGaAs quantum dots separated by GaAs barriers. The waveguide width is 5 $\mu$m and both facets are left as-cleaved leading to a reflectivity of around 32 %. The total laser length is 2 mm corresponding to a free spectral range of around 20 GHz. The laser is mounted on a copper cooling block and temperature stabilized at 20°C. In the lasers with doped active region, the GaAs barriers have been p-doped with concentrations up to $3 \cdot 10^{17}\, cm^{-3}$. Table 1 summarizes all investigated devices with their specific total length to absorber section length ratio. Pulsed laser emission analysis is carried out by a nonlinear intensity auto-correlation technique for pulse width analysis and by de-convolution of Gaussian fits to the measured data (as depicted in Figure 1, right graph) and a fast photo diode (electrical bandwidth 45 GHz) in combination with an electrical spectrum analyzer (electrical bandwidth 50 GHz) for radio-frequency analysis and an optical spectrum analyzer (spectral resolution 10 pm) for optical spectra and bandwidth analysis in dependence on the gain injection current and absorber reverse bias voltage. The timing stability of the optical pulse trains is quantified by the pulse-to-pulse timing jitter $\sigma_{\text{ptp}} = (\Delta\nu/2\pi\nu_0^3)^{0.5}$ with $\nu_0$ being the fundamental repetition rate and $\Delta\nu$ the repetition rate line width [21, 20].

**Table 1.** List of investigated 2 mm long two-section quantum dot laser structures

| number | doping | ridge width | total length to absorber length ratio |
|---|---|---|---|
| 1 | undoped | 5 $\mu$m | 12 % |
| 2 | undoped | 5 $\mu$m | 8 % |
| 3 | undoped | 5 $\mu$m | 5 % |
| 4 | doped | 5 $\mu$m | 12 % |
| 5 | doped | 5 $\mu$m | 5 % |

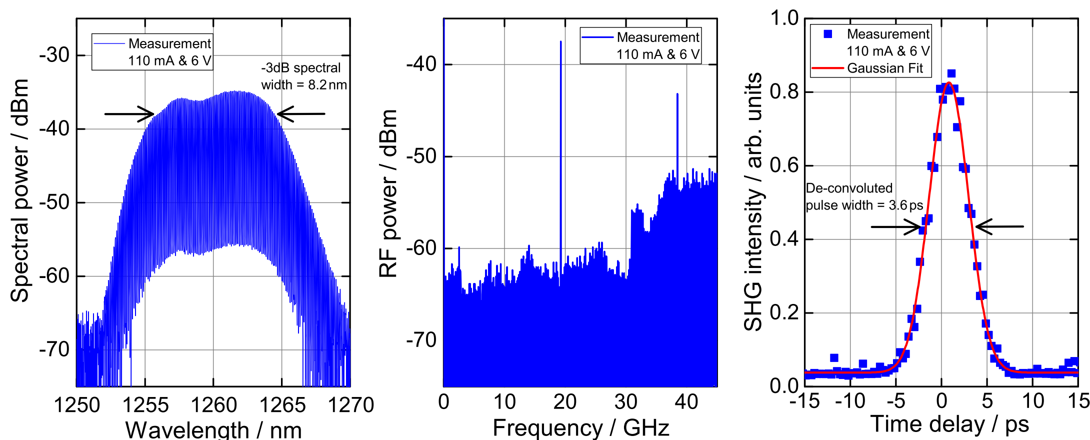


**Figure 1.** Optical spectrum (left), radio-frequency spectrum (middle) and non-linear intensity auto-correlation time trace (right) of undoped laser 1 at a gain injection current of 110 mA and 6 V).

## 3. Experimental results

First, the emission characteristics of lasers 1 and 4 are studied. Exemplary emission characteristics of undoped laser 1 are depicted in Figure 1 at an gain injection current of 110 mA and an absorber reverse bias voltage of 6 V. The -3 dB spectral width of the emitted optical spectrum amounts to 8.2 nm. The middle graph of Figure 1 shows a strong radio-frequency beat note at the fundamental repetition rate whereas a non-linear intensity auto-correlation time trace depicting an optical pulse is depicted in the right graph. The pulse width is determined by a Gaussian fit leading to a value of 3.6 ps at this operation parameters.

The full mapping of the pulse width in dependence on the gain injection current and the absorber reverse bias voltage for undoped laser 1 is depicted in the left graph of Figure 2. The pulse width ranges from 1.3 ps at 65 mA and 6 V up to 25 ps at 305 mA and 3 V. The pulse width is decreasing with increasing absorber reverse bias voltage due to the stronger pulse shortening of the absorber. Additionally, the pulse width is increasing with increasing gain current due to increased self-phase modulation [26]. Those trends are observed for all five laser devices in the fundamental mode-locking regime, independent of the doping or absorber section length, presented in this work. In comparison to undoped laser 1, the resulting pulse width mapping of doped laser 4 is depicted in the right graph in Figure 2. Here, the pulse width ranges from 1.5 ps at 60 mA and 6 V to 30 ps at 210 mA and 4 V. The mode-locking region for the doped sample reduced where mode-locking exists for gain injection currents up to 210 mA. For the undoped device, mode-locking extends up to 305 mA.

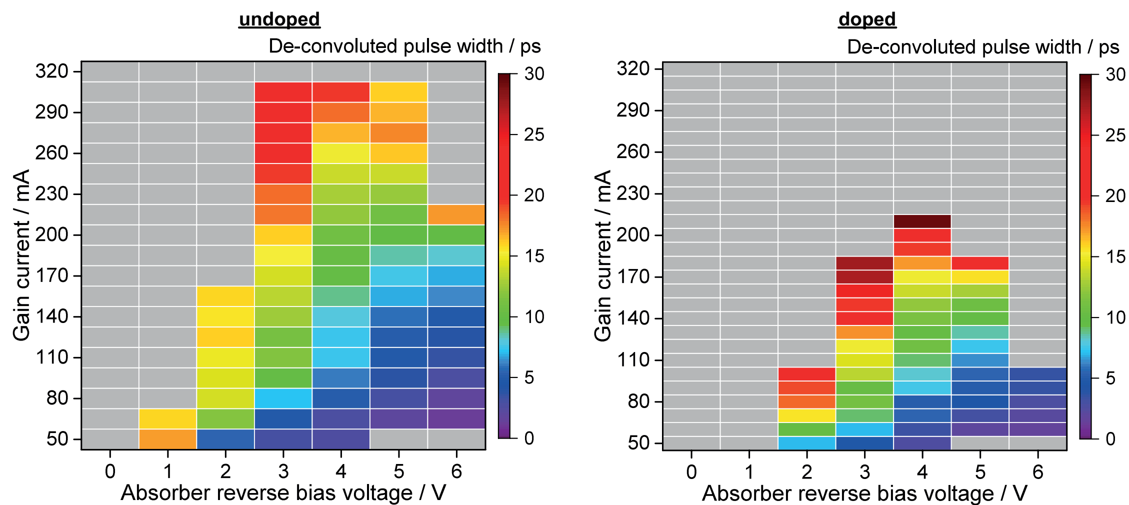


**Figure 2.** Colour-coded pulse width for undoped laser 1 (left) and doped laser 4 (right) in dependence on the gain injection current and absorber reverse bias voltage. In the gray coloured region, continuous wave emission is obtained. At 50 mA and 5 V - 6 V the laser is below threshold. Both lasers are 2 mm long and exhibit total length to absorber section length ratio of 12%.

Second, the shortest pulse widths generated by the laser devices are compared with respect to their absorber section length and doping concentration. Figure 3 depicts the pulse width dependence on the absorber section length ratio for the doped (blue) and undoped (red) lasers. A decrease in shortest pulse width is obtained for both, the doped and undoped lasers for increasing absorber section length. This is in agreement with results recently reported for two-section mode-locked quantum dot lasers on silicon [23]. The shortest pulse width of 1.5 ps generated by the doped laser is slightly higher as compared to the pulse width of 1.3 ps generated by the undoped sample. For a 5% absorber section length, the shortest obtained pulse width of the doped sample is 1.4 times broader and for 12% absorber section length 1.15 times broader

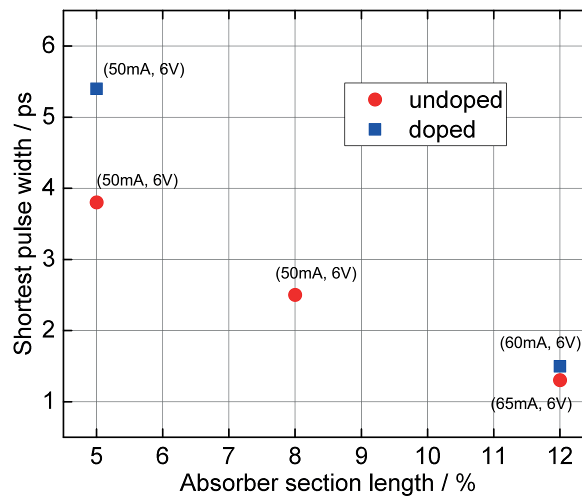


**Figure 3.** Shortest obtained pulse width (including bias conditions) in dependence on the absorber section length to total length ratio of the different laser structures. Red: undoped lasers, blue: doped lasers.

compared to the undoped laser. For the shortest pulse width of 1.3 ps for the undoped device the corresponding timing jitter is 111 fs and for the shortest pulse width of 1.5 ps for the doped device the timing jitter amounts to 2.2 fs showing a more stable pulse train for the doped laser.

Third, harmonic mode-locking is observed for undoped laser 2 (8%) at an absorber reverse bias voltage of 6 V. The evolution of the auto-correlation time traces is depicted color coded in Figure 4. The pulse widths increase from 5.2 ps to 10.1 ps for the laser exhibiting fundamental mode-locking at a repetition rate of 20 GHz and for injection currents from 70 mA to 110 mA. For injection currents ranging from 115 mA to 120 mA the temporal pulse separation amounts

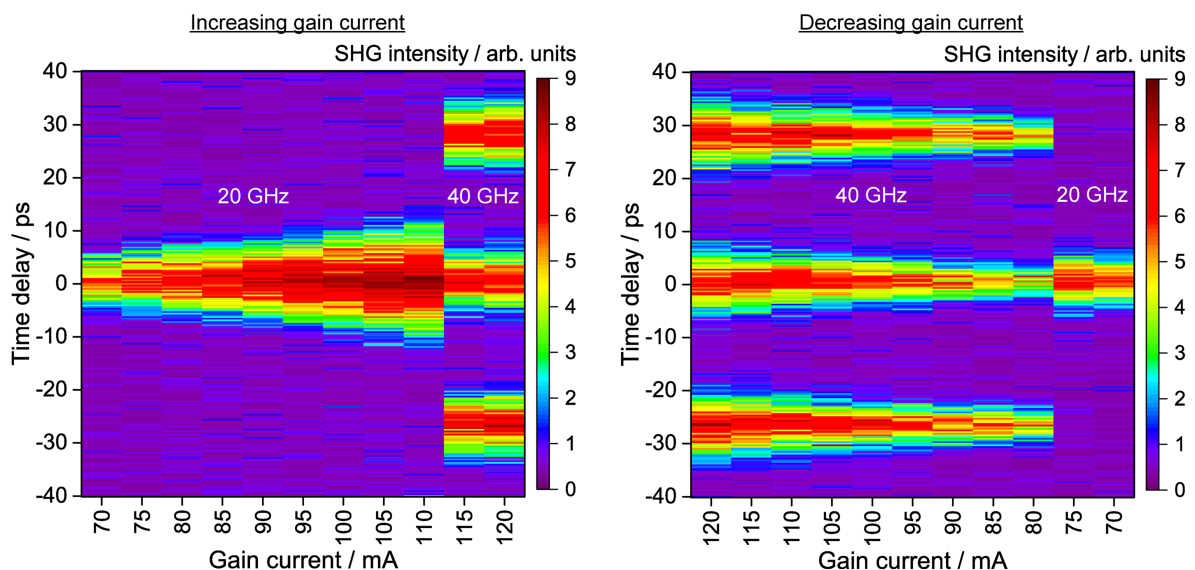


**Figure 4.** Auto-correlation time traces for increasing (left) and decreasing gain current (right) for the undoped 2 mm long laser with an absorber section to total length ratio of 8% operated at at 6 V reverse bias voltage. Repetition rate hysteresis can be found spanning 30 mA.

to 25 ps indicating a repetition rate of 40 GHz. There, two pulses circulate simultaneously in the laser cavity. The laser structures with short absorber section length to total length ratios of 8% and 5% exhibit harmonic mode-locking at absorber reverse bias voltages of 5 V and 6 V. For the short absorber sections the gain at high gain current injection is sufficient to support more than one pulse in the laser cavity. The right graph of Figure 4 shows the auto-correlation time traces for decreasing gain injection currents ranging from 120 mA to 70 mA. Harmonic mode-locking at a repetition rate of 40 GHz extends from 120 mA to 80 mA. At 75 mA the lasers repetition rate transits to fundamental mode-locking at 20 GHz. A repetition rate hysteresis region from 80 mA to 110 mA spanning over 30 mA is evident. Such repetition rate hysteresis effect was already reported in 4 mm long multi-section quantum dot lasers with complex geometry and explained in the context of colliding pulse mode-locking [27].

## 4. Conclusion

In conclusion, the pulsed emission of of 2 mm long two-section passively mode-locked InAs/InGaAs quantum dot lasers has been studied experimentally. The lasers exhibited absorber section length to total length ratios ranging from 5% to 12% and different active region doping. The shortest generated optical pulses amounted to 1.3 ps at a timing jitter of 111 fs generated by an undoped laser with a 12% long absorber. Doped laser device generated pulses with widths as short as 1.5 ps and a timing jitter of 2.2 fs. Active region doping hence leads to increased pulse width yet also higher pulse train stability for those specific devices. Additionally, the undoped device exhibits a larger mode-locking region than the doped device in dependence on the laser biasing conditions. Both the doped and undoped devices with shorter absorber section to total length ratios of 8% or 5% exhibited transitions from fundamental to harmonic mode-locking.

## Acknowledgements

V.V. Korenev, A.V. Savelyev and M.V. Maximov acknowledge support by the Russian Foundation for Basic Research (project #18-502-12081). A.E. Zhukov gratefully acknowledges the support from the Basic Research Program of the National Research University Higher School of Economics 2020. D. Auth and S. Breuer acknowledge support by the Dr. Hans Messer Foundation (Doctoral scholarship); Authors thank W. Elsäßer for support; S. Breuer acknowledges support by the German Research Foundation (DFG) (389193326).

## References

[1] Bimberg D, Kuntz M and Laemmlin M 2005 *Microelectronics Journal* **80** 175–179
[2] Bimberg D, Fiol G, Kuntz M, Meuer C, Lämmlin M, Ledentsov N and Kovsh A 2006 *physica status solidi (a)* **203** 3523 – 3532
[3] Jones R, Doussiere P, Driscoll J B, Lin W, Yu H, Akulova Y, Komljenovic T and Bowers J E 2019 *IEEE Nanotechnology Magazine* **13** 17–26 ISSN 1932-4510
[4] Weber C, Drzewietzki L, Rossetti M, Xu T, Bardella P, Simos H, Mesaritakis C, Ruiz M, Krestnikov I, Livshits D, Krakowski M, Syvridis D, Montrosset I, Rafailov E U, Elsäßer W and Breuer S 2015 *Opt. Lett.* **40** 395–398
[5] Helmchen F and Denk W 2006 *Nature methods* **2** 932–40
[6] Norman J C, Jung D, Wan Y and Bowers J E 2018 *APL Photonics* **3** 030901
[7] Roelkens G, Liu L, Liang D, Jones R, Fang A, Koch B and Bowers J 2010 *Laser & Photonics Reviews* **4** 751–779
[8] V Asryan L and Suris R 1996 *Semiconductor Science and Technology* **11** 554–567
[9] Kuntz M, Fiol G, Laemmlin M, Meuer C and Bimberg D 2007 *Proceedings of the IEEE* **95** 1767–1778 ISSN 0018-9219
[10] Chow W W, Liu A Y, Gossard A C and Bowers J E 2015 *Applied Physics Letters* **107** 171106
[11] Borri P, Schneider S, Langbein W and Bimberg D 2006 *Journal of Optics A: Pure and Applied Optics* **8** S33–S46
[12] Mee J K, Raghunathan R, Wright J B and Lester L F 2014 *Journal of Physics D: Applied Physics* **47** 233001
[13] Matthews D R, Summers H D, Smowton P M and Hopkinson M 2002 *Applied Physics Letters* **81** 4904–4906

[14] Rafailov E, Cataluna M and Avrutin E A 2011 *Quantum Dot Saturable Absorbers* (John Wiley & Sons, Ltd) chap 4, pp 77–97 ISBN 9783527634484
[15] Thompson M G, Rae A R, Xia M, Penty R V and White I H 2009 *IEEE Journal of Selected Topics in Quantum Electronics* **15** 661–672 ISSN 1077-260X
[16] Rafailov E, Cataluna M and Sibbett W 2007 *Nature Photonics* **1** 395–401
[17] Meinecke S, Drzewietzki L, Weber C, Lingnau B, Breuer S and Lüdge K 2019 *Scientific Reports* **9** 1783
[18] Liu S, Wu X, Jung D, Norman J C, Kennedy M J, Tsang H K, Gossard A C and Bowers J E 2019 *Optica* **6** 128–134
[19] Auth D, Liu S, Norman J, Bowers J E and Breuer S 2019 *Opt. Express* **27** 27256–27266
[20] Drzewietzki L, Breuer S and Elsäßer W 2013 *Opt. Express* **21** 16142–16161
[21] Kefelian F, O'Donoghue S, Todaro M T, McInerney J G and Huyet G 2008 *IEEE Photonic. Tech. L.* **20** 1405–1407 ISSN 1041-1135
[22] Carpintero G, Thompson M G, Penty R V and White I H 2009 *IEEE Photonics Technology Letters* **21** 389–391 ISSN 1041-1135
[23] Liu S, Norman J, Jung D, Kennedy M, C Gossard A and Bowers J 2018 *Applied Physics Letters* **113** 041108
[24] Zhang Z, Jung D, Norman J C, Patel P, Chow W W and Bowers J E 2018 *2018 IEEE International Semiconductor Laser Conference (ISLC)* pp 1–2 ISSN 0899-9406
[25] Smowton P M, Sandall I C, Liu H Y and Hopkinson M 2007 *Journal of Applied Physics* **101** 013107
[26] Todaro M, Tourrenc J P, Hegarty S, Kelleher C, Corbett B, Huyet G and Mcinerney J 2006 *Optics letters* **31** 3107–9
[27] Birkholz M, Javaloyes J, Nikiforov O, Weber C, Lester L F and Breuer S 2018 *Semiconductor Lasers and Laser Dynamics VIII* vol 10682 ed Panajotov K, Sciamanna M and Michalzik R International Society for Optics and Photonics (SPIE) pp 235 – 243